



This is a repository copy of *Nonlinear dynamic analysis and control design of a solvent-based post-combustion CO2 capture process*.

White Rose Research Online URL for this paper:  
<http://eprints.whiterose.ac.uk/132998/>

Version: Accepted Version

---

**Article:**

Wu, X., Shen, J., Li, Y. et al. (3 more authors) (2018) Nonlinear dynamic analysis and control design of a solvent-based post-combustion CO2 capture process. *Computers and Chemical Engineering*, 115. pp. 397-406. ISSN 0098-1354

<https://doi.org/10.1016/j.compchemeng.2018.04.028>

---

**Reuse**

This article is distributed under the terms of the Creative Commons Attribution-NonCommercial-NoDerivs (CC BY-NC-ND) licence. This licence only allows you to download this work and share it with others as long as you credit the authors, but you can't change the article in any way or use it commercially. More information and the full terms of the licence here: <https://creativecommons.org/licenses/>

**Takedown**

If you consider content in White Rose Research Online to be in breach of UK law, please notify us by emailing [eprints@whiterose.ac.uk](mailto:eprints@whiterose.ac.uk) including the URL of the record and the reason for the withdrawal request.



[eprints@whiterose.ac.uk](mailto:eprints@whiterose.ac.uk)  
<https://eprints.whiterose.ac.uk/>

# Nonlinear dynamic analysis and control design of a solvent-based post-combustion CO<sub>2</sub> capture process

Xiao Wu<sup>a,\*</sup>, Jiong Shen<sup>a</sup>, Yiguo Li<sup>a</sup>, Meihong Wang<sup>b,\*</sup>,  
Adekola Lawal<sup>c</sup>, Kwang Y. Lee<sup>d</sup>

<sup>a</sup>Key laboratory of Energy Thermal Conversion and Control of Ministry of Education, Southeast University, Nanjing 210096, China

<sup>b</sup>Department of Chemical and Biological Engineering, University of Sheffield, Sheffield S1 3JD, UK

<sup>c</sup>Process Systems Enterprise Ltd, 26-28 Hammersmith Grove, London W6 7HA, UK

<sup>d</sup>Department of Electrical and Computer Engineering, Baylor University, One Bear Place #97356, Waco, TX 76798-7356, USA

## Abstract

A flexible operation of the solvent-based post-combustion CO<sub>2</sub> capture (PCC) process is of great importance to make the technology widely used in the power industry. However, in case of a wide range of operation, the presence of process nonlinearity may degrade the performance of the pre-designed linear controller. This paper gives a comprehensive analysis of the dynamic behavior and nonlinearity distribution of the PCC process. Three cases are taken into account during the investigation: 1) capture rate change; 2) flue gas flowrate change; and 3) re-boiler temperature change. The investigations show that the CO<sub>2</sub> capture process does have strong nonlinearity; however, by selecting a suitable control target and operating range, a single linear controller is possible to control the capture system within this range. Based on the analysis results, a linear model predictive controller is designed for the CO<sub>2</sub> capture process. Simulations of the designed controller on an MEA based PCC plant demonstrate the effectiveness of the proposed control approach.

Keywords: Solvent-based post-combustion carbon capture; Dynamic behavior variations; Nonlinearity investigation; Gap-metric; Model predictive control

## 1. Introduction

Solvent-based post-combustion CO<sub>2</sub> capture (PCC) provides the most mature and feasible technology to remove CO<sub>2</sub> from fossil fuel fired power plant (FFPP) flue gas [1]. Many PCC pilot plants have been built and put into use in recent years; nevertheless, the huge heat consumption for lean-solvent regeneration during the operation is still the main obstacle that limits the PCC application. For this reason, extensive studies, such as equipment and solvent selection [2]-[5], system configuration changes [6]-[8], parameter settings [4], [5], and etc. have been undertaken to improve the efficiency of the process through steady-state optimizations.

Recently, the idea of flexible operation has been promoted and identified as a key technique for the PCC to be widely applied in the power industry. The so called flexible operation is mainly reflected in the following two aspects:

1) as the energy consumption for the CO<sub>2</sub> capture is high, the PCC plants have to change the capture rate flexibly in a wide range, so that the tradeoff between power generation and CO<sub>2</sub> reduction can be made rapidly;

2) as the FFPPs participate in the grid power regulation frequently [9], the flue gas to be treated by the PCC process will have a large variation in mass flow rate, therefore, the PCC plants should flexibly adapt to this flue gas flow rate variation.

In order to achieve a flexible operation of the PCC process, much attention has been paid on the dynamic behavior investigations and control system developments. In Lawal et al. [10], dynamic modeling and simulations on a single absorber model was performed and the results showed that the behavior of the absorber is closely related to the ratio between lean solvent flow rate and flue gas flow rate. Ziaii et al. [11] developed a model for the amine regenerative system, and investigated through simulations the influences of re-boiler heat duty and solvent flow rate on the lean solvent loading.

To provide a thorough understanding of the integrated PCC process dynamics, first principle models were established using different simulation softwares, such as gPROMS [12], [13], Aspen Dynamics [14],[15], Modelica [16], Matlab [17] and gCCS [18], [19]. Bootstrap aggregated neural network model [20] and nonlinear autoregressive exogenous (NLARX) model [21] of the PCC processes were also developed through the identifications from input-output operating data. Based on these models, numerous simulations were then performed and the transient influences of flue gas flow rate/composition, rich/lean solvent flow rate, re-boiler heat duty, etc., on the CO<sub>2</sub> capture rate and thermal energy consumption were fully analyzed. Their results provide

\* Corresponding author.

E-mail address: wux@seu.edu.cn (X. Wu); Meihong.Wang@sheffield.ac.uk (M. Wang)

45 useful information for the control system design.

46 However, although nonlinear differential equations or nonlinear identification approaches are used in all of these studies to  
47 approximate the dynamics of the PCC process [10]-[21], there is no quantification of the nonlinearity level of the PCC process  
48 over a wide range of operation. Important issues for controller design, such as how the nonlinearity is distributed and how the  
49 process dynamics are changed along the considered operating range are still not addressed.

50 On the basis of the dynamic studies, many control designs have been proposed to improve the flexibility of the PCC system  
51 operation. Since the PCC process is highly nonlinear, it is a natural idea to use the nonlinear controllers to achieve a satisfactory  
52 control performance. In [22] and [23], nonlinear analytical models were developed for the integrated PCC process for the NMPC  
53 design purpose, and the models were further simplified to make the computation faster. Although a superior wide range load  
54 variation can be achieved by the NMPC, the nonlinear optimization solving a large number of differential equations lacks  
55 computational robustness and is time consuming. Moreover, an accurate nonlinear control model is difficult to be developed. For  
56 these reasons, linear control approaches attracted much attention and were extensively studied for the PCC process in recent  
57 years.

58 Lawal et al. [12], [13] and Lin et al. [14] both proposed a PI based control structure for the PCC processes. The lean solvent  
59 flow rate and extracted steam flow rate were selected as the primary manipulated variables to control the CO<sub>2</sub> capture rate and  
60 re-boiler temperature, respectively. Simulation verifications demonstrated that such a design can attain a quick control of the  
61 capture rate even in the presence of flue gas flow rate change and CO<sub>2</sub> concentration change. In Lin et al. [15], another control  
62 structure was proposed, which used the lean solvent loading to control the CO<sub>2</sub> capture rate while keeping the lean solvent flow  
63 rate constant. Such a design was shown to have better hydraulic stability in the absorber and stripper, but was not practical,  
64 because lean solvent loading cannot be used as a manipulated variable. Nittaya et al. [24] investigated the interactions among  
65 multi-variables within the PCC system through Relative Gain Array (RGA) analysis. The input-output variables which have the  
66 strongest relationship were paired in one control loop. A 6-input 6-output PI control system was then developed to control the  
67 key variables within the PCC process. In [25] to [27], energy consumption is optimized through steady-state calculation, and  
68 according to the results, the variables which are closely related to the economic performance of the PCC process were selected as  
69 controlled variables, and proper PI control loops were then designed to control these variables.

70 Besides the aforementioned linear PI control loops, linear MPCs have also been applied in the PCC process to achieve a better  
71 flexible control performance. In Bedelbayev, Greer and Lie [28], a linear MPC was designed for the standalone absorber column.  
72 The model was established through linearizing the nonlinear analytical model at a given operating point. Simulation results  
73 show that the MPC can attain a smooth capture rate tracking and quick response to the flue gas flow rate variation. In [29], two  
74 linear MPCs were devised in a double-layer optimal solvent regeneration control system to achieve a fast track of the optimal  
75 re-boiler pressure, the level of solvent in the re-boiler and CO<sub>2</sub> molar flow rate set-points. In [30]-[33] multivariable linear MPCs  
76 were developed to control the key variables of the integrated PCC process. Owing to the outstanding advantages of MPC in  
77 handling strong coupling, slow response and constraint issues, their results all showed that superior performance can be attained  
78 by these linear MPCs compared to the PI/PID based control configurations.

79 However, because the PCC process has a strong nonlinearity along the whole operating range, the system dynamics between  
80 the operating point and the design point may have huge difference. In this case, the presence of nonlinearity will degrade the  
81 performance of designed linear controller severely or even cause the closed-loop system unstable. Although the robustness of the  
82 controllers is tested in some regards, without understanding the nonlinearity level and its distribution along the considered  
83 operating range, the applicable range for the linear controllers is still not clear. Therefore, these linear controllers can only be  
84 used in a small range around the design point and cannot meet the requirement of wide range load variation.

85 In Wu et al. [34], a multi-model predictive controller was designed for the PCC system. Three linear MPCs developed at 50%,  
86 80% and 95% capture rates were combined together to overcome the nonlinearity issue and achieve a wide range capture rate  
87 change control. The flue gas flow rate was considered as an additional measured disturbance in the local model identification, so  
88 that a fast response can be made by the predictive control system in the presence of flue gas flow rate change. Although the  
89 nonlinearity level of the PCC process along the CO<sub>2</sub> capture rate side and flue gas flow rate side was investigated, the  
90 nonlinearity caused by the re-boiler temperature change was not studied. In addition, how the PCC system dynamic changes  
91 under the variation of main parameters and how to effectively avoid the dynamic changes during the operation are not analyzed.

Given these reasons, this paper gives a thorough investigation of the dynamic behavior and nonlinearity distributions of the PCC process. Step response tests are performed at different operating points to illustrate the dynamic variations of the PCC process qualitatively. The method of gap-metric [35]-[40], which is a measurement for the distance between two local linear models is then used to present the nonlinearity level of the PCC system quantitatively. The variations of three main variables along the desired operating range are taken into account: the CO<sub>2</sub> capture rate, the flue gas flow rate and the re-boiler temperature. These three variables are the most important ones closely related to the flexible and efficient operation of the PCC system. It will be shown that, according to the investigation results, the PCC process does have very strong nonlinearity; however, by selecting a suitable control target and operating range, a single linear controller is possible to control the capture system within this range.

Based on the dynamic behavior and nonlinearity analysis results, a linear model predictive controller (MPC) is designed to achieve a flexible operation of the CO<sub>2</sub> capture process. The linear MPC can track the desired CO<sub>2</sub> capture rate quickly and smoothly in a wide range while maintaining the re-boiler temperature tightly around the given point. Moreover, by considering the power plant flue gas flow rate as a measured disturbance in the model development, the proposed MPC can alleviate the impact of flue gas flow rate variation effectively. Simulations on an monoethanolamine (MEA) based post combustion CO<sub>2</sub> plant developed on gCCS demonstrate the conclusions of this paper.

## 2. System Description

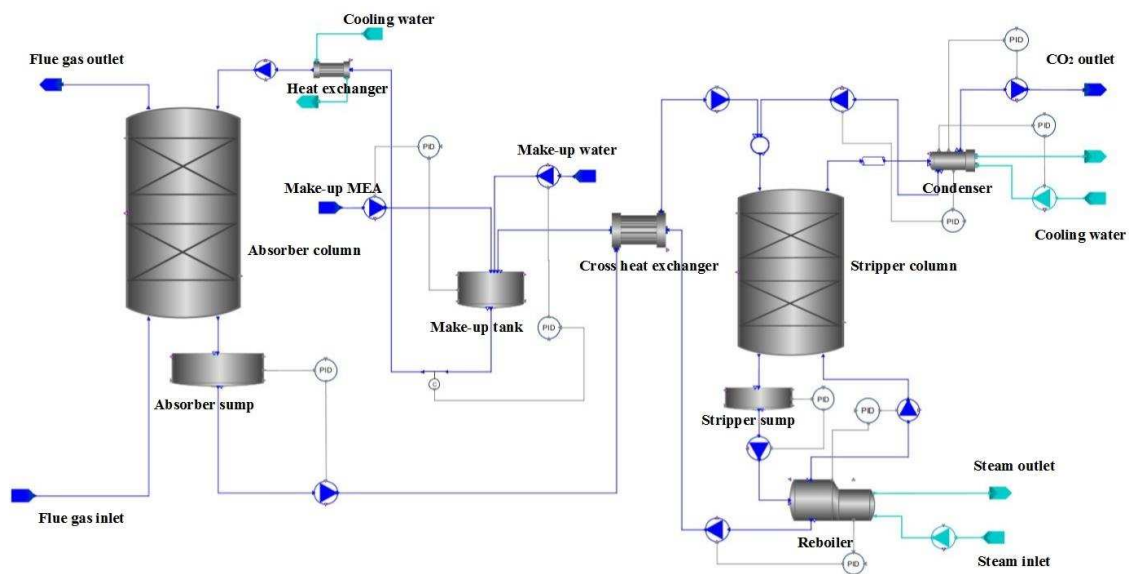


Fig. 1. Schematic diagram of solvent-based PCC process developed on the gCCS platform [18].

The PCC process under consideration is matched with a 1MWe coal-fired power plant, which can produce 0.13 kg/s flue gas (CO<sub>2</sub> concentration: 25.2 wt%) at full load condition. After going through some pre-treatment units, the flue gas is fed into the bottom of the packed-bed absorber column and contact with the chemical solvent counter currently. In this process, CO<sub>2</sub> is absorbed chemically by the solvent and the exited gas is released into the atmosphere from the top side of absorber. Next, the CO<sub>2</sub>-enriched solvent is pumped into the stripper across a lean/rich heat exchanger, where it is heated by steam extracted from the medium/low-pressure turbine of power plant to release the CO<sub>2</sub>. A condenser is then used to recollect the fugitive steam and MEA, the remaining high purity CO<sub>2</sub> is compressed and transported to storage.

The 30 wt% MEA solvent is used as the CO<sub>2</sub> sorbent in this work. The specifications of the main equipments, such as absorber, stripper, re-boiler, condenser and cross heat exchanger are selected according to the model developed in [13], which has been validated through operating data of a pilot capture plant. To provide a high-fidelity description of the PCC process, the model of these devices are developed from the first-principles and then connected based on the working process of CO<sub>2</sub> capture using the gCCS toolkit [18], [19]. The process topology of the PCC model developed in gCCS is presented in Fig. 1.

Within the PCC system, two variables are of the highest importance, the CO<sub>2</sub> capture rate and the reboiler temperature. The CO<sub>2</sub> capture rate is defined as

$$\text{CO}_2 \text{ Capture Rate} = \frac{\text{CO}_2 \text{ in the flue gas} - \text{CO}_2 \text{ in the clean gas}}{\text{CO}_2 \text{ in the flue gas}} \quad (1)$$

The capture rate indicates whether the capture system can fulfill the carbon capture task according to the environmental protection requirements. The re-boiler temperature is closely related to the lean solvent loading, which determines the CO<sub>2</sub> absorption ability of the solvent, and an excessively high temperature will cause a solvent degradation. For these reasons, these two variables need to be tightly controlled [12]-[14], [30]-[34]. The lean solvent flowrate and turbine extracted steam flow rate are usually chosen to control them.

For the flexible operation of the PCC plant, a wide range change of the CO<sub>2</sub> capture rate and a satisfactory adaptation to the power plant flue gas flow rate variation are two basic requirements. Meanwhile, during the dynamic regulation, significant variation of the re-boiler temperature may also have occurred, bringing great influence on the system operation. Therefore, to provide a guidance for the flexible operation of the PCC process, the following operating range is taken into account and nonlinearity level and dynamic behavior variation within this range is analyzed: 1) the CO<sub>2</sub> capture rate is changed between 50%-95%; 2) the flue gas flow rate is changed between 0.07kg/s-0.15kg/s; and 3) the re-boiler temperature is changed between 383K-388K.

For all other variables within the system, such as sump tank level, re-boiler/condenser pressure, and so on, the conventional PI controllers are designed to maintain them closely around their given set-points.

### 3. Nonlinear Dynamic Analysis for the PCC process

To give a comprehensive analysis for the nonlinear dynamics of the solvent-based post-combustion CO<sub>2</sub> capture process, two approaches are used in this section. Firstly, open-loop step response tests are performed at different operating points to show the variation of dynamic behavior and give a qualitative analysis for the nonlinearity distribution; secondly, the approach of gap metric is used to measure the difference in dynamics between two operating points and thus, a quantitative description for the nonlinearity distribution of the PCC process can be obtained.

#### 3.1. Investigation for the dynamic behavior variation of the PCC process

Open-loop step response tests are carried out at different operating points over a wide range of operation to show the variations in dynamic behavior of the PCC process qualitatively. During each step response test, the control loops of capture rate-lean solvent flow rate and re-boiler temperature-steam flow rate are kept open. The other control loops within the gCCS simulator are remained closed to make sure that the PCC plant is operating normally.

To put all the step response curves in the same benchmark for clear comparison, at different operating points, step signals in magnitude of +5% of the respective steady-state values are added to the lean solvent flow rate, steam flow rate and flue gas flow rate channels. To prevent the system from deviating too far away from the investigated point, the magnitude of the step change cannot be too large. The relative changes of capture rate and re-boiler temperature based on their initial steady-state values are then calculated and plotted. The experiments can be divided into three groups: i) investigate the dynamics of PCC system under different capture rates at given flue gas flow rate and re-boiler temperature operating points; ii) investigate the dynamics of PCC system under different flue gas flow rates at given capture rate and re-boiler temperature operating points; and iii) investigate the dynamics of PCC system under different re-boiler temperatures at given capture rate and flue gas flow rate operating points.

Some results are shown in Figs. 2-4.

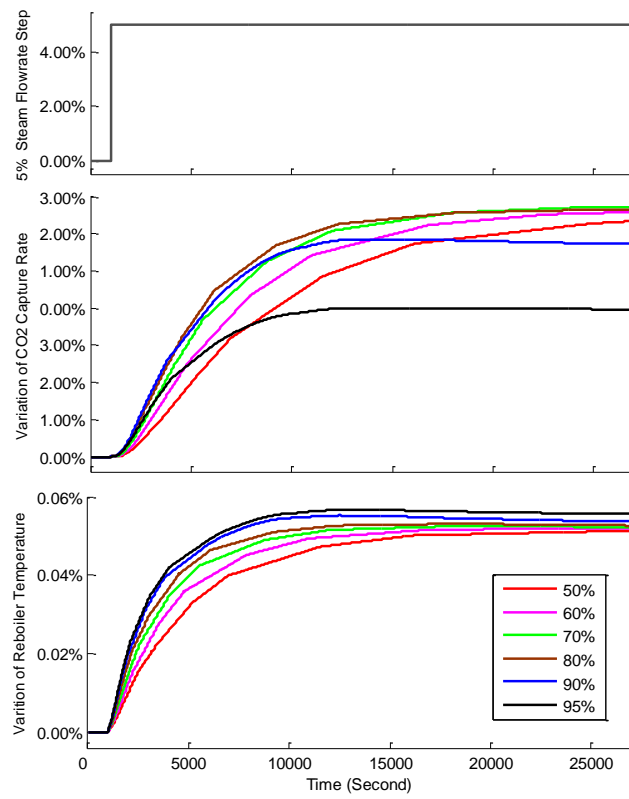


Fig. 2. Responses of the PCC process at different CO<sub>2</sub> capture rates corresponding to steam flow rate step input.

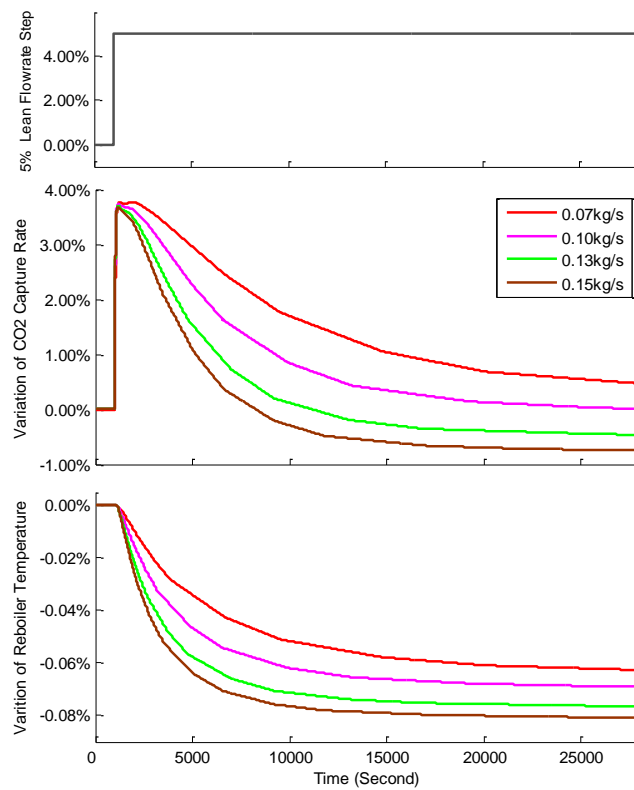


Fig. 3. Responses of the PCC process at different flue gas flow rates corresponding to lean solvent flow rate step input.

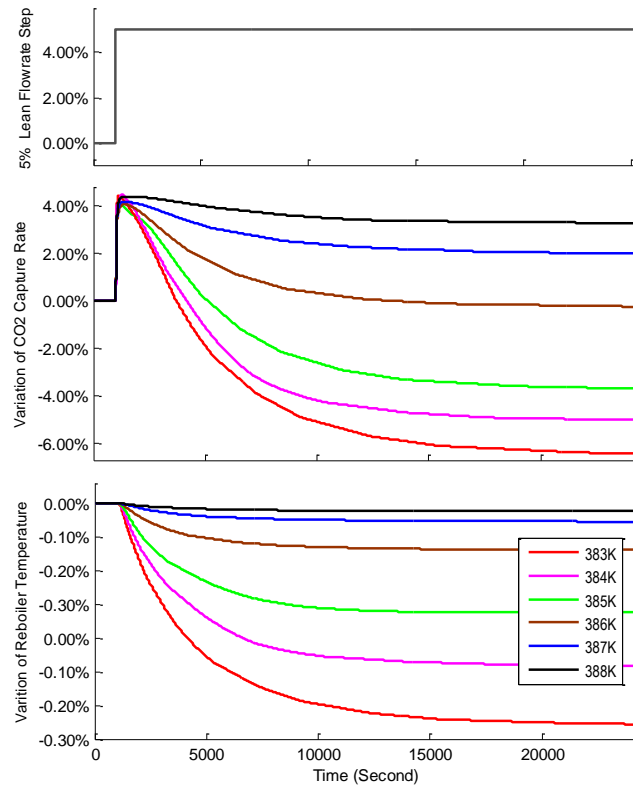


Fig. 4. Responses of the PCC process at different re-boiler temperature corresponding to lean solvent flow rate step input.

Fig. 2 shows the responses of the PCC process at different CO<sub>2</sub> capture rates corresponding to steam flow rate step input (For all tests, the flue gas flow rate is fixed at 0.13kg/s and the re-boiler temperature is set as 386K initially). The change of extracted steam flow rate from turbine will change the re-boiler temperature first, and then change the lean solvent loading which determines the CO<sub>2</sub> absorption ability of the lean solvent. As a result, the CO<sub>2</sub> capture rate will be changed eventually. We can find from the figure that, the influences of the steam flow rate on the re-boiler temperature and capture rate are very slow, which brings difficulties for the flexible operation of the PCC system.

The step response tests also show the variation of dynamic behavior of the PCC system at different CO<sub>2</sub> capture rates. Within 50%- 90% capture rate, we find that the dynamic variation of the system is quite small, the time constants of the system are similar and the steady-state gains only have slight increases as the capture rate increases. Nevertheless, the system dynamics at 95% capture rate is much different from other capture rates. The reason is that: as most of the CO<sub>2</sub> in the flue gas has been gradually captured, it becomes much more difficult for the solvent to absorb the remaining CO<sub>2</sub>, compared with the conditions of other capture rates. The change of rich solvent loading is therefore limited, resulting in a more increase of re-boiler temperature.

The lean solvent flow rate step responses of the PCC process under different flue gas flow rates are then shown in Fig. 3 (For all tests, the CO<sub>2</sub> capture rate and the re-boiler temperature are set as 80%, 386K initially). Because more solvent is sent into the absorber, the increase of lean solvent flow rate can quickly increase the CO<sub>2</sub> capture rate. However, since the steam supplied to the re-boiler does not change, the re-boiler temperature will then drop, as a result, less CO<sub>2</sub> will be stripped off from the solvent and the loading of the lean solvent to the absorber will rise. Finally, the CO<sub>2</sub> capture rate will drop after a while. Although temporary, the quick influence of lean solvent flow rate makes it useful to improve the flexible operation of PCC process. Meanwhile, the non-minimum phase behavior of the lean solvent flow rate-CO<sub>2</sub> capture rate loop may also bring in challenges for the conventional PI control design.

From Fig. 3, we can find that under different flue gas flow rate, the dynamic behavior of the PCC process is also different. This is mainly shown on the steady state gains of the step responses, which is slightly increased as the flue rate flow rate increases. The time constants of the system under different flue gas flow rate are very similar.

Then we show Fig. 4 to illustrate the variation of dynamic behavior of the PCC system at different re-boiler temperatures (For all tests, the CO<sub>2</sub> capture rate is set as 80% initially and the flue gas flow rate is fixed at 0.13kg/s). For the responses of CO<sub>2</sub>

capture rate, the test results show that within 383K-385K operating range, the dynamic variation of the PCC system is limited in terms of steady-state gain and time constant. However, when the temperature rises above 386K, the dynamics of the system become quite different. For a step increase of the lean solvent flow rate, the capture rate no longer drops to a lower level, but returns to the previous level ultimately at 386K operating point, then rises to a higher level at 387K and 388K operating points. For the re-boiler temperature responses, the variation of steady-state gain is also relatively bigger.

At other operating points, the influence of these three variables on the PCC system dynamics is similar to the above results, and thus is not shown here. We can have the following conclusions for the system nonlinearity through these tests:

1) For an individual change of CO<sub>2</sub> capture rate, the system nonlinearity is weak within 50-90% capture rate, but around 95% capture rate, the system nonlinearity is very strong;

2) The system nonlinearity is weak for an individual change of flue gas flow rate; and

3) For an individual change of re-boiler temperature, the system nonlinearity is weak within 383K-385K and 387K-388K operating ranges, however, within 385K-387K operating range the system nonlinearity is strong. (It should be noted that, 385K-387K is a suitable range for the efficient operation of the PCC system according to the steady-state calculation results, and 386K is the optimal re-boiler temperature.)

### 3.2. Nonlinearity analysis of the PCC process via gap-metric

The step response tests show the variations in the dynamic behavior of the PCC system and give a qualitative analysis for its nonlinearity distribution. In order to investigate the level of nonlinearity of the system more concretely and systematically, a quantitative approach, the gap-metric, is proposed to analyze nonlinearity distribution of the PCC process over the operating range.

The gap metric was first introduced to analyze the robust stability of closed-loop uncertain systems [35], [36] and was then extended by Anderson et al. [37] to determine an appropriate model set on which a set of controllers were designed for a multiple model adaptive control. The gap metric method has been successfully applied in multi-model modeling/control of power plant boiler-turbine unit [38], [39] and spacecraft attitude control [40], providing directions for operating region division and local model selection, so that a least number of linear models can be used to approximate the nonlinear behavior of the plant. Most recently, the gap metric was used to quantify the nonlinearity of PCC system along CO<sub>2</sub> capture rate side and flue gas flow rate side using [34]. As an extension to this work, in this paper, the nonlinearity distribution along the re-boiler temperature side is also studied, since the re-boiler temperature is a key variable and may also be changed during the flexible operation of PCC process. Moreover, the nonlinearity caused by the combined variation of these variables is investigated.

The gap metric is essentially a measure of the "distance" between two linear systems, which can be defined as follows:

Suppose  $P_1$  and  $P_2$  are two linear systems, the gap metric between  $P_1$  and  $P_2$  is calculated as:

$$\delta(P_1, P_2) = \max \left\{ \inf_{Q \in H_\infty} \left\| \begin{bmatrix} M_1 \\ N_1 \end{bmatrix} - \begin{bmatrix} M_2 \\ N_2 \end{bmatrix} Q \right\|_\infty, \inf_{Q \in H_\infty} \left\| \begin{bmatrix} M_2 \\ N_2 \end{bmatrix} - \begin{bmatrix} M_1 \\ N_1 \end{bmatrix} Q \right\|_\infty \right\} \quad (2)$$

where  $(N_1, M_1)$ ,  $(N_2, M_2)$  are the elements of the normalized right coprime factorization of  $P_1$  and  $P_2$  as:

$$P_1 = N_1 M_1^{-1}, P_2 = N_2 M_2^{-1}.$$

The gap metric value is bounded between 0 and 1, and a large value represents a major difference between the dynamics of two linear models, thus reflects a strong nonlinearity between these two systems.

To give a comprehensive understanding for the nonlinearity distribution of the PCC process over an operating range (CO<sub>2</sub> capture rate: 50%-95%; flue gas flow rate: 0.07kg/s-0.15kg/s; re-boiler temperature: 383K-388K), local linear models at specified operating points are developed first for gap metric calculation.

At each operating point, random identification signal within  $\pm 2\%$  variation of the steady-state value is applied on the lean solvent flow rate and steam flow rate paths, generating the corresponding output signals. Because the identification signal is closely bounded around their steady-state values, the output variations of CO<sub>2</sub> capture rate and re-boiler temperature can be limited within  $\pm 5\%$  and  $\pm 0.5K$ , respectively, around the operating point. Thus the linear model for a given operating point can



232 be identified from the input-output data. System identification tool box in MATLAB is then used for the local model  
233 identification.

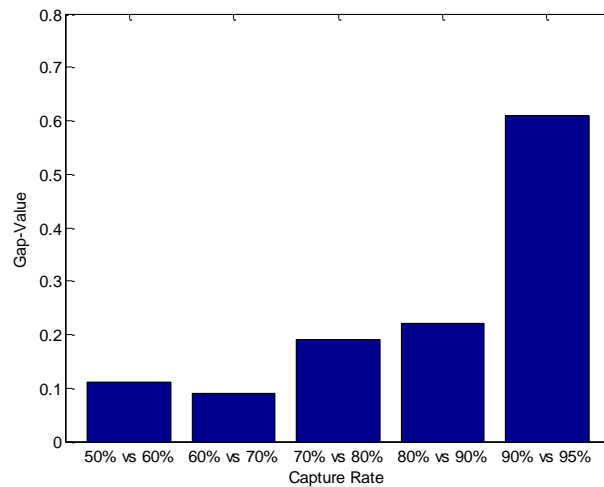
234 We first show Figs. 5-7 to illustrate the nonlinear distribution of the PCC system along the independent variation range of CO<sub>2</sub>  
235 capture rate, flue gas flow rate and re-boiler temperature. Gap metric values between adjacent linear models are calculated to  
236 indicate the nonlinearity level along the corresponding region.

237 To analyze the nonlinearity distribution of the PCC process under the CO<sub>2</sub> capture rate variation. During the local model  
238 identification experiment, we fix the flue gas flow rate at 0.13kg/s and keep the re-boiler temperature around 386K to avoid their  
239 influences. Linear models around 50%, 60%, 70%, 80%, 90% and 95% capture rates are then identified. The gap metric values  
240 calculated between the adjacent linear models are shown in Fig. 5. The results show that within 50%-90% CO<sub>2</sub> capture rate  
241 variation range, the system nonlinearity is weak, however, when the capture rate rises to 95%, the nonlinearity of the PCC  
242 process becomes extremely strong.

243 The nonlinearity distribution of the PCC process under the flue gas flow rate variation is then investigated. During the local  
244 model identification experiment, the CO<sub>2</sub> capture rate and re-boiler temperature are kept around 80% and 386K, respectively, to  
245 avoid their influences. Linear models at 0.07kg/s, 0.10kg/s, 0.13kg/s and 0.15kg/s flue gas flow rate are then identified. The gap  
246 metric values calculated between the adjacent linear models are shown in Fig. 6. The results show that along 0.07kg/s-0.15kg/s  
247 flue gas flowrate variation, the system nonlinearity is weak.

248 For the re-boiler temperature variation, we keep the CO<sub>2</sub> capture rate around 80% and fix the flue gas flow rate at 0.13kg/s  
249 during the local model identification experiment to avoid their influences. Linear models at 383K, 384K, 385K, 386K, 387K, and  
250 388K points are then identified. The gap metric values calculated between the adjacent linear models are shown in Fig. 7. The  
251 results show that between 383K-385K, 387K-388K re-boiler temperature variation ranges, the system nonlinearity is weak;  
252 however, between 385K-387K operating range, the nonlinearity of the PCC process becomes very strong.

253 The nonlinearity analysis results are in strong agreement with the step-response tests results as shown in Section 3.1.



254  
255 Fig. 5. Nonlinearity distribution of the PCC process under the CO<sub>2</sub> capture rate variation.

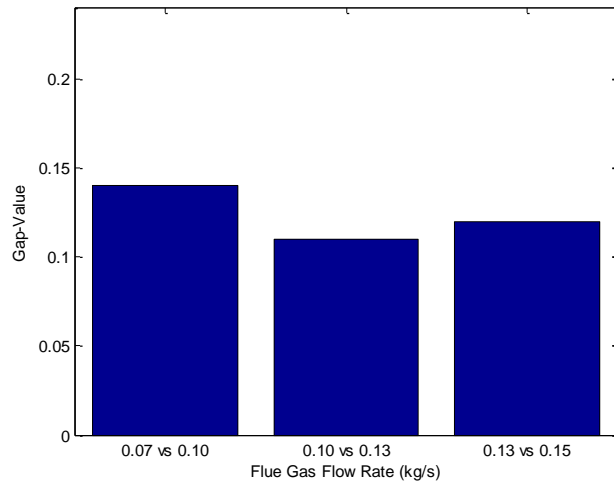


Fig. 6. Nonlinearity distribution of the PCC process under the flue gas flowrate variation.

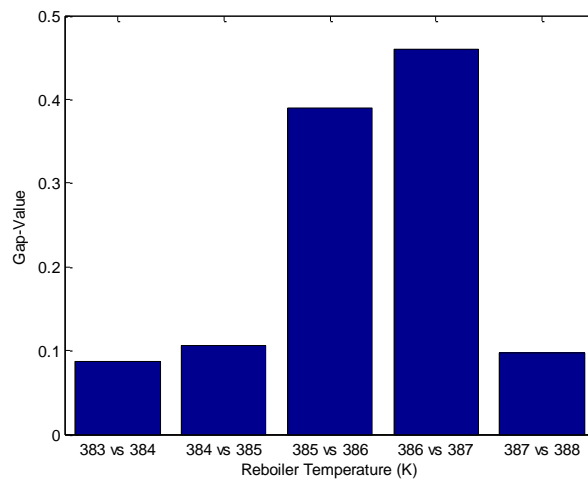


Fig. 7. Nonlinearity distribution of the PCC process under the re-boiler temperature variation.

During the operation of the PCC plant, the CO<sub>2</sub> capture rate, re-boiler temperature and upstream power plant flue gas flowrate may change together. Therefore, it is necessary to investigate the nonlinearity of the PCC system under the combined change of these variables. However, doing this will result in 144 (6×6×4) local models to be identified, which will take a lot of time in excitation signal design and data generation. Moreover, since there are three independent variables and one dependent variable, the nonlinearity strength under the influences of the three variables cannot be displayed intuitively by figures. For this reason, the following two cases are considered to analyze the nonlinearity level of the PCC process:

- 1) The flue gas flowrate is fixed at 0.13kg/s, the CO<sub>2</sub> capture rate varies between 50%-95%, the re-boiler temperature varies between 383K-388 K;
- 2) The re-boiler temperature is fixed at 386K, the CO<sub>2</sub> capture rate varies between 50%-95%, the flue gas flow rate varies between 0.07kg/s-0.15kg/s.

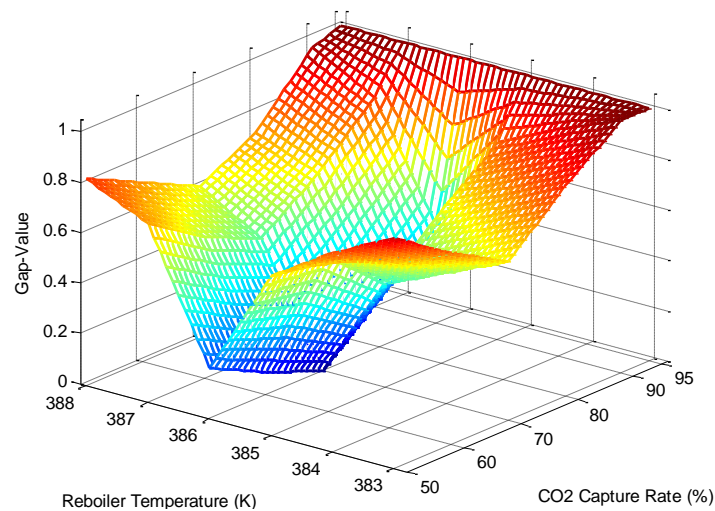


Fig. 8. Nonlinearity distribution of the PCC process under the variations of CO<sub>2</sub> capture rate and re-boiler temperature.

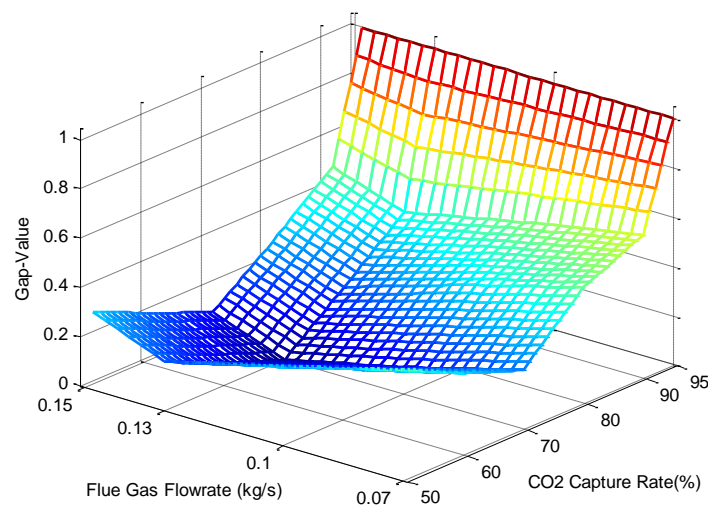


Fig. 9. Nonlinearity distribution of the PCC process under the variations of CO<sub>2</sub> capture rate and flue gas flow rate.

In both two cases, the linear models identified at (80% capture rate, 0.13kg/s flue gas flow rate, 386K re-boiler temperature) operating point is set as a benchmark. Gap metric values between other local models and the benchmark model are then calculated as shown in Figs. 8 and 9 to display the nonlinearity level of the PCC process.

The results show that the PCC process does have very strong nonlinearity; when the operating point deviates far away from the benchmark point, the gap metric value keeps increasing. As shown in Fig. 8, within 50%-95% capture rate, 385-387K re-boiler temperature range (efficient operating range of the plant), the gap-metric value of the PCC system changes drastically as the re-boiler temperature changes, indicating that the system nonlinearity is strong within this range for an independent variation of re-boiler temperature. The change of CO<sub>2</sub> capture rate will further increase the nonlinearity to a higher level, however, when the capture rate is varied within 50%-90% range, its impact on the system nonlinearity is limited. On the other hand, Fig. 9 shows that within 50%-90% capture rate, 0.07kg/s-0.15kg/s flue gas flow rate operating range, the gap-metric value of the PCC system changes quite smoothly. This means a combined variation of CO<sub>2</sub> capture rate and flue gas flow rate will not bring too much nonlinearity to the PCC system within this range. The nonlinearity analysis results provide a useful information that, if the re-boiler temperature can be tightly controlled around the given operating point, a linear controller may be possible to achieve a satisfactory performance for the flexible operation of PCC process.

#### 4. Linear Control Design for the Flexible Operation of the PCC process

For the nonlinear PCC process, it is a natural idea to design a nonlinear controller to attain a whole operating range control of

292 the PCC system. However, solving the nonlinear control algorithm is complex. The computational process is time-consuming  
 293 and the calculation results are poor in robustness. For this reason, linear controller is still the first choice in process control  
 294 design. As depicted in Section 3, the PCC process do have very strong nonlinearity; nevertheless, if the re-boiler temperature is  
 295 well controlled around a given set-point, the nonlinearity of the process will become much weaker, thus a linear controller may  
 296 become possible to regulate the PCC process within 50%-90% CO<sub>2</sub> capture rate range.

297 To overcome the difficulties of the PCC process operation, such as large inertial behavior and strong couplings among  
 298 multi-variables, a linear model predictive controller is developed for the flexible operation of the PCC plant. A linear state-space  
 299 model around 70% CO<sub>2</sub> capture rate, 386K re-boiler temperature operating point is identified as the prediction model, thus by  
 300 solving a simple quadratic programming (QP), the constrained control action can be quickly calculated. To further intensify the  
 301 adaptation ability of the PCC system to the variation of flue gas flowrate, the flue gas flowrate is considered as a measured  
 302 disturbance in the prediction model. Thus its influence on the PCC process can be quickly alleviated. The prediction model used  
 303 in the MPC design is shown as

$$304 \begin{cases} \mathbf{x}_{k+1} = \mathbf{A}\mathbf{x}_k + \mathbf{B}\mathbf{u}_k + \mathbf{E}\mathbf{d}_k \\ \mathbf{y}_k = \mathbf{C}\mathbf{x}_k + \mathbf{D}\mathbf{u}_k + \mathbf{F}\mathbf{d}_k \end{cases} \quad (3)$$

305 where  $\mathbf{u}_k = [u_{1k} \quad u_{2k}]^T$  is the input vector composed by the lean solvent flowrate  $u_1$  and turbine extracted steam flowrate  $u_2$ ,  
 306  $\mathbf{y}_k = [y_{1k} \quad y_{2k}]^T$  is the output vector composed by the CO<sub>2</sub> capture rate and re-boiler temperature,  $\mathbf{d}_k$  is the flue gas flowrate,  $\mathbf{x}_k$  is  
 307 the state vector; A, B, C, D, E, F are the model matrices identified from operation data, which are listed in the Appendix.

308 Because the control objective is to track the CO<sub>2</sub> capture rate to the desired point, maintain the re-boiler temperature at a given  
 309 set-point and meanwhile keep the control actions as smooth as possible. The following dynamic objective function is considered:

$$310 J = (\hat{\mathbf{y}}_f - \mathbf{r}_f)^T \mathbf{Q}_f (\hat{\mathbf{y}}_f - \mathbf{r}_f) + \Delta \mathbf{u}_f^T \mathbf{R}_f \Delta \mathbf{u}_f \quad (4)$$

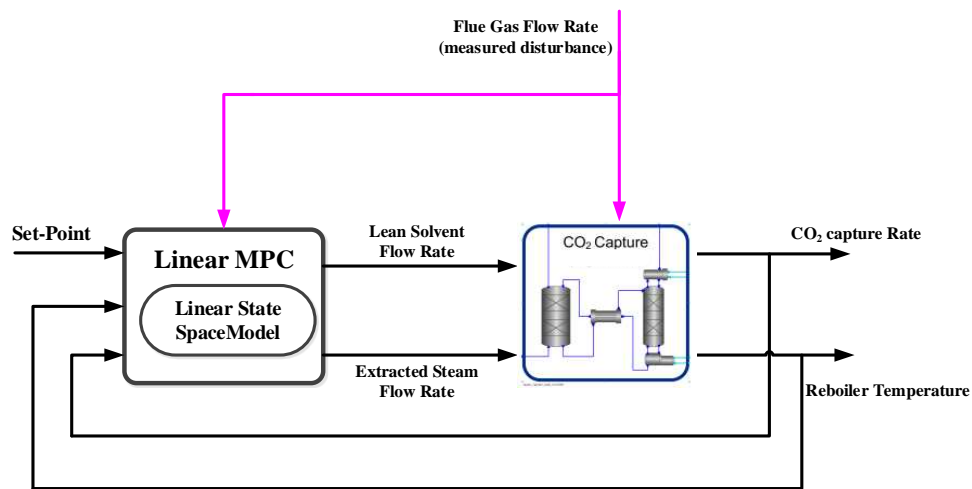
311 where  $\hat{\mathbf{y}}_f = [\hat{y}_{k+1}^T \quad \hat{y}_{k+2}^T \quad \cdots \quad \hat{y}_{k+N_y}^T]^T$  is the prediction of future output within the predictive horizon  $N_y$ , which can be expressed

312 by the future input sequence by stacking up the predictive model (3);  $\mathbf{r}_f = [r_{k+1}^T \quad r_{k+2}^T \quad \cdots \quad r_{k+N_y}^T]^T$  is the desired output

313 set-points;  $\Delta \mathbf{u}_f$  is the increment of future control input sequence  $\mathbf{u}_f = [u_{k+1}^T \quad u_{k+2}^T \quad \cdots \quad u_{k+N_u}^T]^T$  on the control horizon  $N_u$ ;

314  $\mathbf{Q}_f = \mathbf{I}_{N_f} \otimes \mathbf{Q}_0$ ,  $\mathbf{R}_f = \mathbf{I}_{N_u} \otimes \mathbf{R}_0$ ,  $\otimes$  presents the Kronecker product, are the weighting matrices of output and input, respectively.

315 At each sampling time, minimizing the control objective function (4) subject to some input magnitude and rate constraints, the  
 316 optimal future control sequence  $\mathbf{u}_f$  can be calculated. The first element in  $\mathbf{u}_f$ ,  $u_{k+1}$ , can then be implemented on the PCC system  
 317 [35]. The schematic diagram of the proposed MPC is shown in Fig. 10.



318  
 319 Fig.10. Schematic diagram of the proposed MPC for the solvent-based post-combustion CO<sub>2</sub> capture system.

320

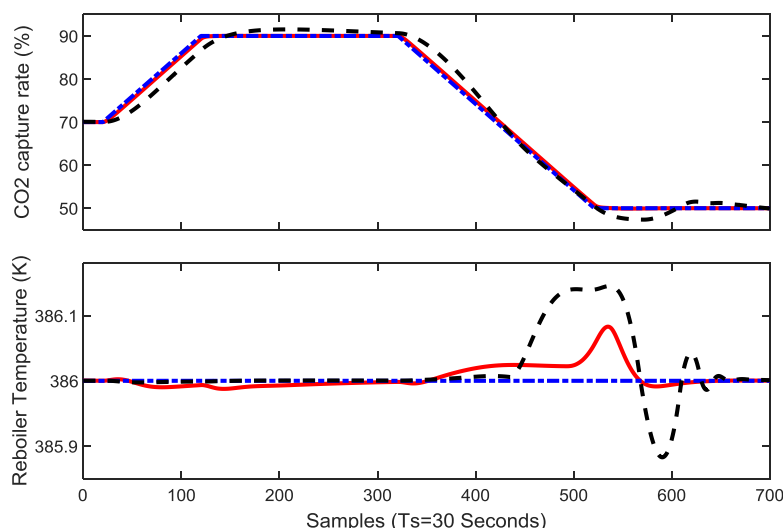
321 **5. Simulation Results**

322 This section presents simulation results which will be able to demonstrate the effectiveness of the linear MPC for the flexible  
 323 operation of the PCC process. The following parameters are set for the MPC: sampling time  $T_s=30s$ , predictive horizon  $N_y=600s$ ,  
 324 control horizon  $N_u=150s$ ; the weighting matrices are set as  $Q_0=\text{diag}(5, 1)$ ;  $R_0=1000 \times \text{diag}(3, 2)$ . Input magnitude and rate  
 325 constraints are considered:  $u_{\min} = [0.2 \quad 0.005]^T$ ,  $u_{\max} = [1 \quad 0.08]^T$ ;  $\Delta u_{\min} = [-0.007 \quad -0.001]^T$ ,  $\Delta u_{\max} = [0.007 \quad 0.001]^T$  due to  
 326 the physical limitations of the valves and pumps.

327 The linear MPC are devised and run in the MATLAB environment, it is communicated with the gCCS plant model through the  
 328 gOMATLAB interface at each sampling time. Another decentralized PI controller which uses the lean solvent flow rate to control  
 329 the CO<sub>2</sub> capture rate and uses the steam flow rate to control the re-boiler temperature is designed for comparison purpose. The  
 330 parameters are tuned at 70% capture rate, 386K re-boiler temperature operating point using the MATLAB PID Tuner toolbox.

331 Case 1: the first simulation is used to show the effectiveness of the linear MPC in the flexible regulation of CO<sub>2</sub> capture rate.  
 332 Suppose that the PCC system is operating at 70% capture rate point initially, then at  $t=600s$  and  $t=9600s$ , the set-point of capture  
 333 rate changes to 90% and 50% at the ramping rate of 0.2%/30s according to the instruction of scheduling. The re-boiler  
 334 temperature set point is fixed at 386K. The simulation results are shown in Figs. 11 and 12.

335



336

337 Fig. 11. Performance of the PCC system for a 70%-90%-50% CO<sub>2</sub> capture rate change: output variables (solid in red: MPC; dashed in black: decentralized PI;  
 338 dot-dashed in blue: reference).

339

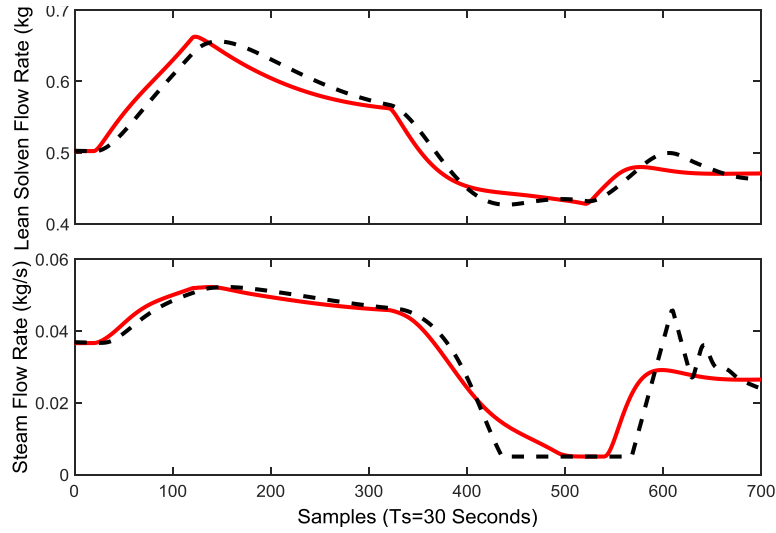


Fig. 12. Performance of the PCC system for a 70%-90%-50% CO<sub>2</sub> capture rate change: manipulated variables (solid in red: MPC; dashed in black: decentralized PI).

For the slow dynamics of PCC system as shown in Figs. 2-4, the results in Figs. 11 and 12 indicate that, the use of proposed MPC can greatly improve the response speed of the entire closed-loop system and achieve an excellent control performance. When the CO<sub>2</sub> capture rate set-point changes in a wide range, the controller can quickly regulate the lean solvent flow rate, making the capture rate follow the desired set-point tightly and smoothly. At the same time, the extracted steam flow rate is optimized accordingly with the lean solvent flow rate to provide a suitable regeneration thermal energy. The re-boiler temperature is thus controlled closely around the designed point, guaranteeing an efficient operation of the PCC plant and avoiding the influence of strong nonlinearity on the model predictive control system.

For the decentralized PI controller, it can also attain a satisfactory performance. It once again demonstrates that: if the re-boiler temperature can be maintained well, linear controller is capable to achieve a wide range control within 50%-90% CO<sub>2</sub> capture rate range. However, since the decentralized PI control cannot handle the PCC behavior of slow dynamics and coupling, its control performance is worse than the MPC. The CO<sub>2</sub> capture rate tracking speed is slower and the re-boiler temperature also has larger fluctuations.

Case 2: The second simulation is designed to demonstrate the effectiveness of the linear MPC in flexible adaptation to the flue gas flow rate variation. We assume that the PCC plant is operating at 70% capture rate operating point, at t=600s and t=7500s, the flue gas flow rate changes from 0.13kg/s to 0.07kg/s and to 0.15kg/s, respectively, as shown in the upper figure of Fig. 13. The set-points for CO<sub>2</sub> capture rate and re-boiler temperature are fixed at 70% and 386K during the simulation.

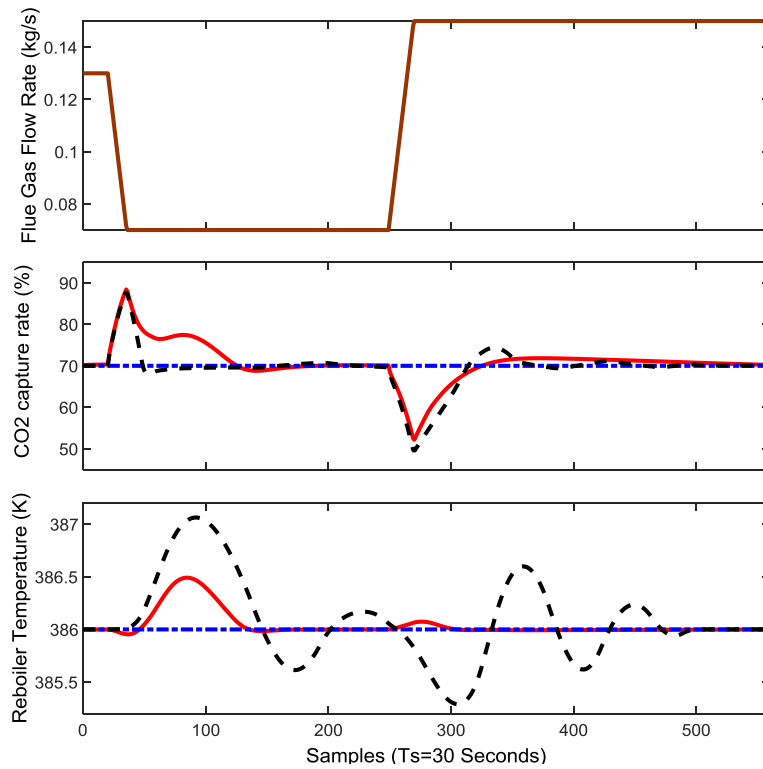


Fig. 13. Performance of the PCC system in the presence of power plant flue gas variation: output variables (solid in red: MPC; dashed in black: decentralized PI; dot-dashed in blue: reference).

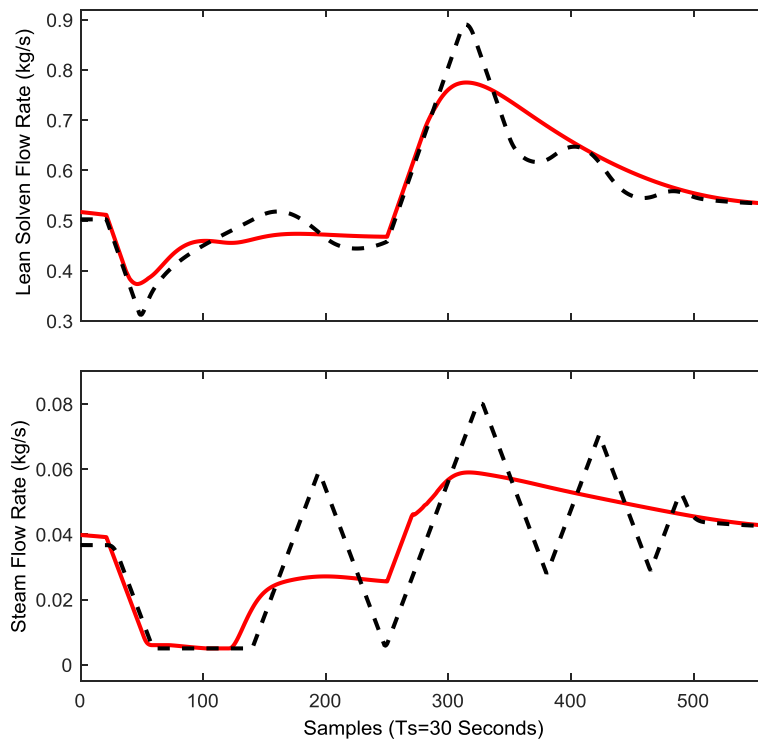


Fig. 14. Performance of the PCC system in the presence of power plant flue gas variation: manipulated variables (solid in red: MPC; dashed in black: decentralized PI).

The simulation results in Figs. 13 and 14 demonstrate that the proposed MPC can effectively handle the impact of flue gas flow rate variation. As defined in equation (1), when the flue gas flow rate changes drastically, a large deviation immediately occurred for the CO<sub>2</sub> capture rate control. However, since the flue gas flow rate is considered in the model development, a good prediction can be made in the presence of flue gas flow rate variation. The MPC quickly adjusts the lean solvent flow rate and extracted steam flow rate, force the CO<sub>2</sub> capture rate back to the set-point while alleviating the re-boiler temperature fluctuation

370 as much as possible. It is also interested to note that when the flue gas decreases from 0.13 kg/s to 0.07kg/s, the control effect is  
371 worse than that the flue gas increases from 0.07 kg/s to 0.15kg/s. This is mainly due to the restriction of magnitude and rate  
372 constraints during the reduction of extracted steam flow rate.

373 On the other hand, the performance of decentralized PI controller is much worse. The main reason is that, the completely  
374 decentralized design cannot take into account the coupling effects among the multi-variables, adjust the lean solvent flow rate  
375 and re-boiler steam flow rate coordinately. When the flue gas flow rate changes, the capture rate quickly shows a large control  
376 offset. As a result, the lean solvent flow rate changes greatly, trying to control the capture rate quickly back to the set-point.  
377 However, the excessive variation of lean solvent flow rate causes large fluctuations in re-boiler temperature, which will then  
378 make system dynamics change and thus further degrade the control performance. It can be seen in Fig. 14 that both the lean  
379 solvent flow rate and re-boiler steam flow rate exhibit certain degrees of vibrations, which is extremely unfavorable to the safe  
380 operation of the PCC system.

381 The simulations fully illustrate the effectiveness of the MPC in the flexible operation of the solvent-based post- combustion  
382 CO<sub>2</sub> capture process. They also show that, by maintaining the re-boiler temperature closely around the given set-point, a linear  
383 controller is possible to achieve a 50%-90% capture rate change for the PCC plant and adapt flexibly to the flue gas flowrate  
384 variation.

## 385 6. Conclusion

386 To provide guidance for the controller design and achieve a flexible operation of the solvent-based post-combustion CO<sub>2</sub>  
387 capture process, this paper gives a thorough investigation for the dynamic behavior variation and nonlinearity distribution of the  
388 PCC process. Three cases are taken into account during the investigation, the CO<sub>2</sub> capture rate variation, the power plant flue gas  
389 flow rate variation and the re-boiler temperature variation. Step response tests at different operating points are performed to  
390 display the dynamic variation of the PCC system qualitatively. The gap-metric values between local models at different operating  
391 points are then calculated to show the nonlinearity distribution of the system quantitatively.

392 The analysis results show that: 1) Within 50%-90% CO<sub>2</sub> capture rate range, the nonlinearity level of the PCC process is weak,  
393 however, when the capture rate rises to 95%, the nonlinearity becomes strong; 2) the system nonlinearity caused by the variation  
394 of flue gas flow rate is very limited; and 3) the system nonlinearity can be extremely strong with the variation of re-boiler  
395 temperature within 385K-387K, which is the efficient operating range of the PCC system. The strong nonlinearity within this  
396 range does not mean that we must abandon the optimal operating temperature of 386K. Instead, we must avoid the severe  
397 fluctuation of the re-boiler temperature during the operation, so that the issue of nonlinearity can be overcome.

398 Therefore, according to these results, the requirement for re-boiler temperature control should be strengthened in the controller  
399 design. If the re-boiler temperature can be well maintained around a given set-point, linear controllers are possible to well  
400 regulate the CO<sub>2</sub> capture rate within 50% and 90% operating range, avoiding the solving issues of nonlinear controller. A linear  
401 model predictive controller is thus designed to achieve a quick regulation for the CO<sub>2</sub> capture rate and good maintenance for the  
402 re-boiler temperature. To improve the MPC's adaptation to the flue gas flow rate variation, the flue gas flow rate is considered as  
403 a measured disturbance in the prediction model development. In this way, an accurate model prediction can be made even in the  
404 presence of flow gas flow rate change and its influence can be quickly removed by the MPC. Simulation results on an MEA  
405 based post combustion CO<sub>2</sub> capture plant demonstrate the effectiveness of the linear control approach.

## 406 Acknowledgements

407 The authors would like to acknowledge the National Natural Science Foundation of China (NSFC) under Grant 51506029, the  
408 Natural Science Foundation of Jiangsu Province, China under Grant BK20150631, China Postdoctoral Science Foundation, EU  
409 FP7 International Staff Research Exchange Scheme on power plant and carbon capture (Ref: PIRSES-GA-2013-612230).

## 410 Appendix

411 System matrices of the predictive model (identified around 70% capture rate, 386K re-boiler temperature point, sampling time:  
412 Ts=30s):



$$\begin{aligned}
A &= \begin{bmatrix} 1.0000 & 0.0026 & 0.0034 & -0.0001 \\ 0.0000 & 0.9972 & 0.0048 & 0.0462 \\ 0.0000 & 0.0009 & 0.9878 & 0.0771 \\ 0.0000 & -0.0076 & 0.0165 & 0.4261 \end{bmatrix}, B = \begin{bmatrix} 0.0317 & -0.3874 \\ 0.8037 & 0.4409 \\ 1.5411 & -1.8324 \\ -11.2252 & 10.6440 \end{bmatrix}, \\
C &= \begin{bmatrix} -0.0035 & 0.0618 & -0.0048 & -0.2000 \\ -1.7123 & 0.0200 & 0.0266 & -0.0067 \end{bmatrix}, D = \begin{bmatrix} 0.8885 & 0.1630 \\ -0.0634 & 0.8252 \end{bmatrix}, \\
E &= \begin{bmatrix} -0.0134 \\ -0.8191 \\ -1.2170 \\ 9.6344 \end{bmatrix}, F = \begin{bmatrix} -4.0242 \\ 0.0827 \end{bmatrix}.
\end{aligned}$$

The model is stable since no eigenvalues of A matrix are located out of the unit circle. The D matrix is not null because the sampling time of data collection is selected as  $T_s=30s$ . Within the period of 30 seconds, the changes of MVs have already caused the variations of CVs (especially lean-solvent flow rate to  $CO_2$  capture rate), which can be shown in Figs. 2-4.

## References

- [1] IEA. Energy Technology Perspectives 2008. IEA/OECD, Paris, France, 2008.
- [2] J. Oexmann. Post-Combustion  $CO_2$  Capture: Energetic Evaluation of chemical Absorption Processes in Coal-Fired Steam Power Plants. Ph.D. thesis, Technische Universitat Hamburg-Harburg, 2011.
- [3] J. Oexmann, C. Hensel and A. Kather. Post-combustion  $CO_2$ -capture from coal-fired power plants: preliminary evaluation of an integrated chemical absorption process with piperazine-promoted potassium carbonate. International Journal of Greenhouse Gas Control, vol. 2, pp. 539–552, 2008.
- [4] P. Mores, N. Rodríguez, N. Scenna and S. Mussati.  $CO_2$  capture in power plants: Minimization of the investment and operating cost of the post-combustion process using MEA aqueous solution. International Journal of Greenhouse Gas Control, vol. 10, pp. 148–163, 2012.
- [5] A. Raksajati, M. T. Ho and D. E. Wiley. Reducing the cost of  $CO_2$  capture from flue gases using aqueous chemical absorption. Ind. Eng. Chem. Res, vol. 52, no. 47, pp. 16887-16901, Nov 2013.
- [6] M. Karimi, H. F. Svendsen and M. Hillestad. Capital costs and energy considerations of different alternative stripper configurations for post combustion  $CO_2$  capture. Chemical Engineering Research and Design, vol. 89, no. 8, pp. 1229–1236, 2011.
- [7] L. Duan, M. Zhao and Y. Yang. Integration and optimization study on the coal-fired power plant with  $CO_2$  capture using MEA. Energy, vol. 45, pp.107-116, 2012.
- [8] Q. Chen, C. Kang, Q. Xia and D. S. Kirschen. Optimal flexible operation of a  $CO_2$  capture power plant in a combined energy and carbon emission market. IEEE Trans. Power Syst., vol. 27, no. 3, pp.1602-1608, Aug. 2012.
- [9] X. Wu, J. Shen, Y. Li, and K. Y. Lee. Steam power plant configuration, design and control, WIREs Energy Environ, vol. 4, no. 6, pp. 537-563, Nov-Dec. 2015.
- [10] A. Lawal, M. Wang, P. Stephenson and H. Yeung. Dynamic modelling of  $CO_2$  absorption for post combustion capture in coal-fired power plants, Fuel, vol. 88, pp. 2455-2462, 2009.
- [11] S. Ziaii, G.T. Rochelle and T. F. Edgar. Dynamic modeling to minimize energy use for  $CO_2$  capture in power plants by aqueous monoethanolamine, Ind. Eng. Chem. Res, vol. 48, no. 13, pp. 6105-6111, 2009.
- [12] A. Lawal, M. Wang, P. Stephenson and O. Obi. Demonstrating full-scale post-combustion  $CO_2$  capture for coal-fired power plants through dynamic modelling and simulation, Fuel, vol. 101, pp. 115-128, 2012.
- [13] A. Lawal, M. Wang, P. Stephenson, G. Koumpouras and H. Yeung. Dynamic modelling and analysis of post-combustion  $CO_2$  chemical absorption process for coal-fired power plants, Fuel, vol. 89, pp. 2791-2801, 2010.
- [14] Y. Lin, T. Pan, D. Wong and S. Jang. Plantwide control of  $CO_2$  capture by absorption and stripping using monoethanolamine solution. 2011 American Control Conference, San Francisco, CA, USA, Jun 29-Jul 1, 2011.
- [15] Y. Lin, D. Wong, S. Jang and J. Ou. Control strategies for flexible operation of power plant with  $CO_2$  capture plant, AIChE Journal, vol. 58, no. 9, pp. 2697-2704, 2012.
- [16] K. Dietl, A. Joos and G. Schmitz, Dynamic analysis of the absorption/desorption loop of a carbon capture plant using an object-oriented approach,

- 449 Chemical Engineering and Processing: Process Intensification, vol. 52, pp.132-139, 2012.
- 450 [17] S. A. Jayarathna, B. Lie, M. C. Melaen, Amine based CO<sub>2</sub> capture plant: dynamic modeling and simulations. International Journal of Greenhouse Gas  
451 Control, vol. 14, pp. 282-290. 2013
- 452 [18] J. Rodriguez, A. Andrade, A. Lawal, N. Samsatli, S. Calado, T. Lafitte, J. Fuentes and C. Pantelides. An integrated framework for the dynamic modelling  
453 of solvent-based CO<sub>2</sub> capture processes, Energy Procedia vol.63, pp. 1206-1217, 2014.
- 454 [19] E. Mechleri, A. Lawal, A. Ramos, J. Davison and N. M. Dowell. Process control strategies for flexible operation of post-combustion CO<sub>2</sub> capture plants,  
455 International Journal of Greenhouse Gas Control, vol. 57, pp. 14-25, 2017.
- 456 [20] F. Li, J. Zhang, E. Oko and M. Wang. Modelling of a post-combustion CO<sub>2</sub> capture process using neural networks, Fuel, vol. 151, pp. 156-163, 2015.
- 457 [21] N. A. Manaf, A. Cousins, P. Feron and A. Abbas. Dynamic modelling, identification and preliminary control analysis of an amine-based post-combustion  
458 CO<sub>2</sub> capture pilot plant, Journal of Cleaner Production, vol. 113, pp. 635-653, 2016.
- 459 [22] J. Åkesson, C.D. Laird, G. Lavedan, K. Prölb, H. Tummescheit, S. Velut and Y. Zhu. Nonlinear Model Predictive Control of a CO<sub>2</sub> Post-Combustion  
460 Absorption Unit, Chemical Engineering & Technology, vol. 35, no. 3, pp. 445-454, 2012.
- 461 [23] K. Prölb, H. Tummescheit, S. Velut and J. Åkesson. Dynamic model of a post-combustion absorption unit for use in a non-linear model predictive  
462 control scheme, Energy Procedia, vol. 4, 2620-2627, 2011.
- 463 [24] T. Nittaya, P. L. Douglas, E. Croiset and L. A. Ricardez-Sandoval. Dynamic modelling and control of MEA absorption processes for CO<sub>2</sub> capture from  
464 power plants. Fuel, vol. 116, pp. 672-691, 2014.
- 465 [25] M. Schach, R. Schneider, H. Schramm and J. Repke. Control structure design for CO<sub>2</sub>-absorption processes with large operating ranges. Energy  
466 Technology. vol.1, no. 4, pp. 233-244, Apr 2013.
- 467 [26] M. Panahi, S. Skogestad, Economically efficient operation of CO<sub>2</sub> capturing process part I: self-optimizing procedure for selecting the best controlled  
468 variables, Chemical Engineering and Processing: Process Intensification, vol. 50, no.3, pp. 247-253, 2011.
- 469 [27] M. Panahi, S. Skogestad, Economically efficient operation of CO<sub>2</sub> capturing process part II: Design of control layer, Chemical Engineering and Processing:  
470 Process Intensification, vol. 52, pp. 112-124, 2012.
- 471 [28] A. Bedelbayev, T. Greer and B. Lie. Model based control of absorption tower for CO<sub>2</sub> capturing. 49th Scandinavian Conference on Simulation and  
472 Modeling, Oct 2008.
- 473 [29] A. Arce, N. Mac Dowell, N. Shah and L.F. Vega, " Flexible operation of solvent regeneration systems for CO<sub>2</sub> capture processes using  
474 advanced control techniques: Towards operational cost minimisation," International Journal of Greenhouse Gas Control, vol. 11, pp.  
475 236-250, 2012.
- 476 [30] A. Cormos, M. Vasile and M. Cristea, Flexible operation of CO<sub>2</sub> capture processes integrated with power plant using advanced control techniques, 12th  
477 International Symposium on Process Systems Engineering and 25th European Symposium on Computer Aided Process Engineering, Copenhagen,  
478 Denmark, May 31-Jun 4, 2015.
- 479 [31] E. D. Mehleri, N. Mac Dowell and N. F. Thornhill, Model Predictive Control of Post-Combustion CO<sub>2</sub> Capture Process integrated with a power plant, 12th  
480 International Symposium on Process Systems Engineering and 25th European Symposium on Computer Aided Process Engineering, Copenhagen,  
481 Denmark, May 31-Jun 4, 2015.
- 482 [32] Q. Zhang, R. Turton and D. Bhattacharyya, Development of Model and Model-Predictive Control of an MEA-Based Post-combustion CO<sub>2</sub> Capture  
483 Process, Industrial & Engineering Chemistry Research, vol. 55, no. 5, pp. 1292-1308, 2016.
- 484 [33] M. T. Luu, N. A. Manaf and A. Abbas, Dynamic modelling and control strategies for flexible operation of amine-based post-combustion CO<sub>2</sub> capture  
485 systems, International Journal of Greenhouse Gas Control, vol. 39, pp. 377-389, 2015.
- 486 [34] X. Wu, J. Shen, Y. Li, M. Wang and A. Lawal, Flexible operation of post-combustion solvent-based carbon capture for coal-fired power plants using  
487 multi-model predictive control: a simulation study, Fuel, vol. 220, pp. 931-941, 2018.
- 488 [35] T. Georgiou and M. Smith, Optimal Robustness in the Gap Metric, IEEE Transactions on Automatic Control, vol. 35, no. 6, pp. 673-686, 1990.
- 489 [36] L. Qiu, E. J. Davison, Feedback stability under simultaneous gap metric uncertainties in plant and controller. Systems & Control Letters, vol. 18, no. 1, pp.  
490 9-22, 1992.
- 491 [37] B. Anderson, T. Brinsmead, F. Bruyne, J. Hespanha, D. Liberzon, and A. Morse, Multi model adaptive control. Part 1: Finite controller coverings, Int. J.  
492 Robust Nonlinear Control, vol. 10, pp. 909-929, 2000.
- 493 [38] X. Wu, J. Shen, Y. Li, and K. Y. Lee, Data-driven modeling and predictive control for boiler-turbine unit. IEEE Transactions on Energy Conversion, vol. 28,  
494 no.3, pp. 470-81, 2013.
- 495 [39] Y. Li, J. Shen, K. Y. Lee and X. Liu, Offset-free fuzzy model predictive control of a boiler-turbine system based on genetic algorithm, Simulation

496 Modelling Practice and Theory, vol. 26, pp. 77-95, 2012.

497 [40] S. Saki, H. Bolandi and S. Mashhida, Optimal direct adaptive soft switching multi-model predictive control using the gap metric for spacecraft attitude

498 control in a wide range of operating points, Aerospace Science and Technology, vol. 77, pp. 235-243, 2018.

499